IEEE Access
Multidisciplinary : Rapid Review : Open Access Journal

Received 29 June 2023, accepted 14 July 2023, date of publication 19 July 2023, date of current version 3 August 2023.

Digital Object Identifier 10.1109/ACCESS.2023.3296801

RESEARCH ARTICLE

Design and Implementation of a Lightweight Deep CNN-Based Plant Biometric Authentication System

WENQING YAN[1], (Member, IEEE), JINGWEI TANG[2], AND SANDRO STUCKI[1,3]

[1]Institute for Building Materials, ETH Zürich, 8093 Zürich, Switzerland
[2]Department of Computer Science, ETH Zürich, 8092 Zürich, Switzerland
[3]Swiss Federal Laboratories for Materials Science and Technology (Empa), 8600 Dübendorf, Switzerland

Corresponding author: Wenqing Yan (yanw@ethz.ch)

This work was supported in part by the ETH Zürich Career Seed Grant under Grant 1-009041.

ABSTRACT The wide application of personal biometric information such as face, fingerprint, iris, and voiceprint has simultaneously created many new ethical and legal issues, including the fraudulent use of biometrics. A non-human biometric system is demanded as an alternative, which features no human private information and can be replaced or renewed from time to time. The main objective of this study is to identify wood or leaf biometric patterns and verify their identities by building their respective datasets. On this basis, a plant biometric feature-based recognition system and authentication application were developed and implemented by employing a deep convolutional neural network (CNN) architecture to learn the embedding model using a distance-based triplet-loss similarity metric. We used two kinds of small datasets based on wood and leaves, which are Spruce Cross-Section (SCS) dataset and Collinsonia Canadensis Leaf Abaxial Surface (CCLAS) dataset. A series of artificial augmentations have been integrated into training to mimic the changes in the images during the usage of keys in real-world scenarios. The final results achieve accuracy values of 97.56% (validation set) and 96.06% (test set) on the Spruce Cross-Section (SCS) dataset and 99.11% (validation set) and 98.61% (test set) on the Collinsonia Canadensis Leaf Abaxial Surface (CCLAS) dataset, indicating the high reliability of this non-human biometric authentication system.

INDEX TERMS Biometric authentication system, deep learning, leaf biometric recognition, Squeeze-Net, wood biometric recognition.

I. INTRODUCTION

Authentication by human biometric verification has advanced tremendously and is becoming increasingly prevalent in the world today. This encompasses behaviour characteristics such as gait [1], keystrokes [2], signatures [3], [4], specific physiological characteristics like fingerprints [5], [6], [7], facial features [8], iris [9], [10], [11], voice [12], [13], [14], and internal biometric data such as heart rate and breathing [1]. According to the 2021 Global Identity & Fraud Report, although 74% of consumers prefer biometric authentication as the primary security method, users deemed it the least secure [15]. When this intrinsically unique personal biometric data is extensively used on versatile public occasions, it involves more and more security issues. Our biometric data can be leaked or hacked from the database, while replacing or updating it with a new biological feature from time to time is unlikely. Moreover, it is difficult to ensure that the collection, storage and use of biometric data are conducted in accordance with international human rights and privacy laws [16]. In the case of password authentication systems, such as knowledge-based authentication, individuals may encounter difficulties remembering answers due to the wide range of public records and information sources from which the questions are generated. These questions can be distressing as they delve into personal history or past relationships.

The associate editor coordinating the review of this manuscript and approving it for publication was Ines Domingues.

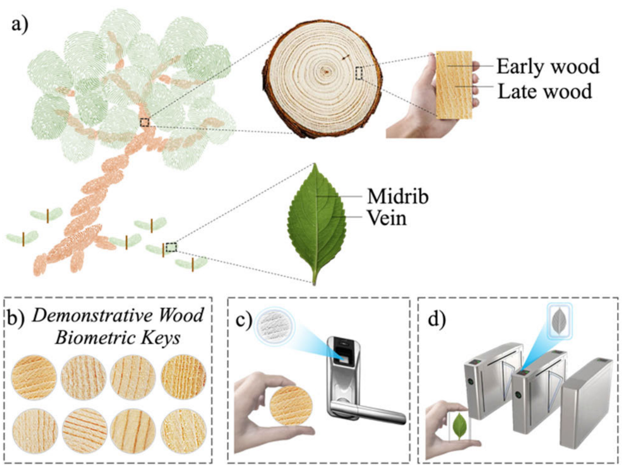

FIGURE 1. a) Schemes and images of biometric features on wood and leaf: a wooden block originated from a wood cross-section, which consists of distinct early woods and late woods; a leaf biometric feature is composed of midribs and veins. b) Demonstrative biometric patterns of wood samples for verification. c) Wood biometric verification for a lock system. d) A "leaf key" for security identification.

Additionally, the use of numbers, letters, or characters as answers can lead to easy leakage during communication or be known by acquaintances. In contrast, biometric patterns are intricate and unique, enhancing security. Due to the high efficiency of human biometric recognition and low system cost, there are different degrees of abuse of face recognition technology in shopping malls, scenic spots, communities, and even at crime scenes. Besides the concern of fraudulent use and leakage, the aging of the biometrics degrades the performance of their recognition algorithms [17].

As a complementary solution, a non-human biological verification system is proposed as an alternative to human biometric recognition. Plant organs and tissues have characteristics that are uniquely identifiable in terms of the form and configuration of their patterning. Like human fingerprints, no two growth ring sequences of wood or two leaves are exactly identical.

Wood, one of the most abundant natural materials, is an ultimate renewable and sustainable resource. The wood biometric pattern features seasonal-generated annual rings of varying width consisting of earlywoods and latewoods with considerable differences in density and width, most pronounced in softwoods and ring-porous hardwoods. The fine structure of wood grain is composed of wood fibers, vessels, and tracheids varying with different arrangement directions, making wood a perfect material for identification (Figure 1a).

Similarly to wood, each leaf is also unique. The essential structure of a leaf features a midrib and branches on each side to produce veins of vascular tissue.

Computer vision (CV)-based identification on wood and leaf features has been making steady progress to meet the needs of the industry and market [18], [19]. Wood or leaf recognition mainly contributes to the science of plant classification, recognition, identification, plant education, or environmental protection and exploration. This presented work has been carried out with the goal of authentication for lock systems and exhibits the following contributions.

- Develop CNN-based wood and leaf biometric recognition systems, as sustainable alternatives to human biometric security systems.
- Assess the feasibility of the proposed system using different evaluation matrices such as accuracy, precision, recall, and F1 score.
- A learning-based method is proposed with an adapted Squeeze-Net for feature extractions and verifications. The model is trained with triplet loss to increase the embedding distance of nonmatch-identity pairs and decrease that of match-identity pairs. A simple decision tree algorithm is adopted for determining the threshold of classification of match- and nonmatch identities.
- Separate image datasets of wood and leaves are created for training. A series of artificial augmentations, such as image enhancement, rotation, and translations, are integrated into training to mimic the changes in the images during the usage of keys in real scenarios.
- This paper presents visualizations of the ground-truth and predicted examples, to interpret the obtained results and analyse the reliability of the models' predictions.

II. RELATED WORK

According to purposes and motivations, research on CV-based wood or leaf identification can be classified as follows: **1) Recognition and classification of species.** Koch et al. demonstrated computer-aided identification and description of trade timbers [20]. Lau and co-workers developed an automated wood species recognition system and achieved a recognition rate of 80.00% [21]. Souza et al. analysed timber sections by using deep learning based on wood timber microscope images with 281 species, which has helped efficiently provide the timber certification and allow the application of correct timber taxing [22]. A new Gabor based wood recognition approach has been demonstrated by researchers based on wood stereogram images, the performance of recognition has been improved by extracting more efficient and effective features from Gabor patterns and carrying out in different areas [23]. Mouine et al. recognized leaf by combining triangular approaches with a shape-context based descriptor, and achieved a high retrieval accuracy [24]. **2) Log traceability.** Uhl and co-workers investigated biometric log recognition using a texture feature-based fingerprint matching technique [25] and evaluated the applicability in real world identification scenarios [26]. To combat the illegal logging more efficiently, a fully automated system has been built by researchers in the same group by applying a CNN-based segmentation and recognition [27]. **3) Surface defect detection.** Wang et al. studied three common defects including dead knots, poles and living knots of wood based on texture features, the highest recognition rate is 91.33% corresponding to the network structure with 12 layers of hidden layers [28]. **4) Identification of disease for certain species.** Fang et al. achieved macroscopic and dynamic detection of pine wood nematode disease with the help of CNN remote sensing methods [29]. Brownspot or other color information were used for leaf disease recognization [30], [31]. **5) Waste recycling.** Researchers in Belgium presented a vision-based solution for such a wood waste sorting system. They applied a classification algorithm to separates medium density fibreboard (MDF), oriented strand board (OSB) and other particleboard (grade B wood) from a mixed wood waste stream [32]. This work has a strong positive impact on the environment.

Among the above-mentioned applications, in the early period, the most frequently used computer vision methods were conventional machine learning methods, which are based on hand-crafted features. These features are manually engineered and can be determined by gray level co-occurrence matrix (GLCM) [33], [34], [35], [36], local binary pattern (LBP) [37], [38], [39], scale-invariant feature transform (SIFT) [40], [41], [42], speeded up robust features (SURF) [43], [44], oriented features-from-accelerated-segment-test (FAST) [43], etc. With the development of deep learning, high-level plant features can be learned by machine automatically from a dataset in an incremental manner. This eliminates the need of manual feature extraction by domain expertise, making CV-based plant identification more widely pervasive. Convolutional neural network (CNN) is the most commonly applied deep neural network technique. Ding et al. used the CNN algorithm to effectively extract the wood defect contour and reached a wood defect recognition accuracy of 96.72% in a test time of only 187ms [45]. Zhou et al. identified wood microscopic images based on CNN's precise wood specification identification model [46]. Jyothi and co-authors proposed a modified version of CNN that constituted multilevel layers and enabled testing on a system with a very small and highly degraded dataset [47]. In order to learn the representative features from the complex diseased leaf images, a three-channel CNN model was constructed by combining three color components, each channel is fed by one of the three color components of the RGB image [31].

Deep learning networks have demonstrated their significance in plant identification, classification, and disease recognition. A highly reliable plant-based biometric authentication system is necessary to meet the needs of the industry and market, simultaneously protecting human private information from fraudulent use and illegal collection.

III. METHODOLOGY

A. SCS AND CCLAS DATASETS

We create two separate datasets for experiments by capturing macroscale RGB images using a mobile phone (HUAWEI P30 Pro). Each image sample has an original size of 3648 × 2736 RGB images. The first dataset utilizes spruce cross-section (SCS, figure 2a, cut by circular saw) planes, and the second one comes from Collinsonia canadensis leaf abaxial surface (CCLAS, figure 2b, obtained from nature). This part of the plant was chosen due to their characteristic textures which are easily distinguishable by modern deep learning methods. The image samples in SCS are cropped to remove unimportant borders outside the object and resized, resulting in images in pixels 899 × 311.

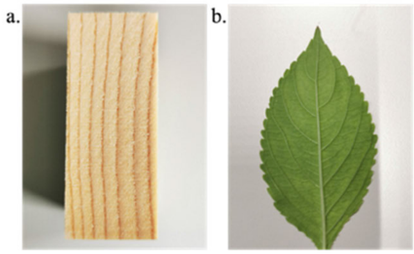

FIGURE 2. a) An exemplary image from SCS system and b) image from CCLAS dataset.

The images in CCLAS are roughly segmented according to colours, and resized to 640 × 320. Examples of the dataset can be seen in Figure 2. Each of the datasets contains three subsets: 200 unique examples for the training set, 20 unique samples for the validation set, and 20 unique samples for the test set. To mimic the real-world key usage scenarios, we randomly place each sample five times in both the validation and test sets, and capture them in varying lighting conditions. This results in effectively 100 samples in both validation and test sets. It is worth noting that for the purpose of saving materials, some independent images from the SCS dataset are from different cross-section planes along the same wood block with a vertical distance as low as 5 cm, which could result in extremely similar textures and add difficulty to verification. These samples account for roughly 50% of the total SCS samples.

B. IMAGE PREPROCESSING AND TRIPLET LOSS

In recent developments in computer vision, several effective convolutional neural network architectures have been developed for image classification purposes [48], [49], [50]. These architectures can usually be seen as general feature extraction combined with one classification layer. In this work, we utilize the feature extraction part of SqueezeNet [51] that is specifically created with a small number of trainable parameters and thus low memory and power consumption for easy incorporation into embedded systems. The input to the network is a 3-channel RGB image of arbitrary size. During training, we always use images of size 320 × 160. A pooling layer is added at the end of the architecture so that the network outputs a 1000-element feature embedding.

The training process aims at encouraging the distances between a pair of feature embeddings with the "same" identities to be smaller than the minimum distance of samples between "different" identities. The triplet loss function [52] developed in face recognition fields is a common way of achieving this purpose:

$$\mathcal{L}=\sum_{i}^{N}\max(\|f(x_i^a)-f(x_i^p)\|_2^2-\|f(x_i^a)-f(x_i^n)\|_2^2+\alpha,0) \tag{1}$$

where a stands for "anchor" sample, p for "positive" sample, and n for "negative" sample. Anchor and positive samples are of the same identity, while anchor and negative samples are of different identities. $f(x)$ is the feature embedding output of the neural network. Margin value α is a hyperparameter. In our experiments, we fix $\alpha = 111.384$.

C. DECISION TREE FOR DISTANCE THRESHOLDING

The training results in the embeddings of the same-identity features being closer and the embeddings of the different-identities being further away. However, to verify whether the incoming wood or leaf is of the same identity as the current wood or leaf, a threshold value of embedding distances is required. If the distance is below the threshold, it is recognized that the incoming sample has the same identity as the current sample, and vice versa.

In this study, a simple decision tree of depth one for thresholding is adopted. The threshold value is computed purely based on (augmented) training examples: all possible pairs in the training set are selected to fit the decision tree. Once fitted, the threshold value can then be used to determine (predict) whether the pairs in the validation or test sets are of the "same" identity (1) or "different" identity (0).

D. DATA AUGMENTATION

To train the network to predict the same image under rotation, translation, and lighting condition variation to have the "same" identity, a series of the above operations for data augmentation are adopted.

In particular, each input image is rotated 0-20 degrees randomly; translated 0%-10% of the total size in both horizontal and vertical directions randomly; flipped horizontally with a probability of 0.5; and adjusted on brightness, contrast, and colour balance with factors sampled from a gaussian distribution of mean 1.0 and standard deviation 0.2. The samples are finally center-cropped and resized to 320×160 as input for training. Examples of augmented samples can be seen in Figure 3.

E. EVALUATION METRICS

The proposed system is primarily evaluated based on four metrics. The system utilized the evaluation metrics for measuring the effectiveness of the proposed system: accuracy, precision, recall, and F1 score.

F. APPLICATION

The application setup has four parts: 1) Wood samples are taken randomly from the test set. 2) The same mobile phone (HUAWEI P30 Pro) is used for image capture. 3) Laptop with CNN identification system in Python. 4) Python lock with both lamp and motor systems. The setup consisted of an Arduino Nano connected to a servo motor (SG90), a red and green LED, and an HC-05 Bluetooth SPP (Serial Port Protocol) module. The setup was powered by a 9-volt battery. The HC-05 was connected to the Arduino and configured in secondary mode to receive commands via Bluetooth. The servo motor was used as a lock. In its ground state, the servo motor is at 0° and locks the lid. Sending a pre-defined unlock signal to the HC-05 activates the green LED and triggers the servo motor to rotate 90° and unlock the lid. If the received signal does not correspond to the unlock signal, the red LED is activated and the lock remains closed.

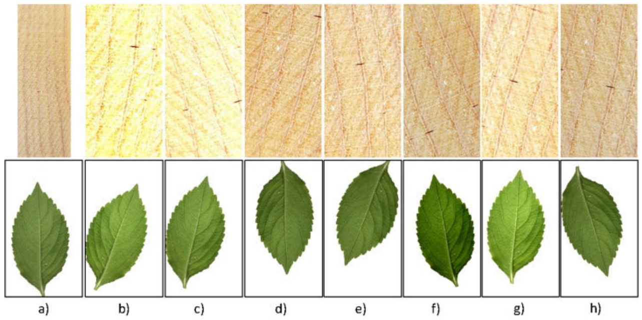

FIGURE 3. Examples from both SCS (top row) and CCLAS (bottom row) dataset. a) is the original sample. b) – h) are augmented samples.

IV. RESULTS AND DISCUSSION

The implementation details of our deep CNN in both training and testing steps will be described in this section. We perform our experiments using the SCS and CCLAS datasets to analyse the verification scenario. The result is compared with other biometric verification systems.

We trained our model on GeForce GTX 1080 Ti (with 11GB of memory size) GPU tools and extensive amounts of data. Figure 4 shows an overview of our model. At training time, input images of different identities (ID_0, …, ID_m) are preprocessed through the data augmentation technique discussed in Section III-D. We created training pairs through combining ID_0 with other identities (ID_1, …, ID_m). Features Embeddings of the images are then extracted by the SqueezeNet Extractor. Triplet loss is subsequently applied to train the neural network. At test time, two images from the camera captures are passed through the feature extractor to get the embedding. The decision tree decides if they are of the same identity based on the embedding distances.

A. TRAINING OF SQUEEZE-NET ON A TRIPLET LOSS FUNCTION

For detailed testing settings, the model supervised with triplet loss is evaluated on the datasets. Figure 5 presents the probability density of the wood biometric system by using different margins. There are some overlaps in distances between 100 and 200. This can be improved through better network design and sample generation.

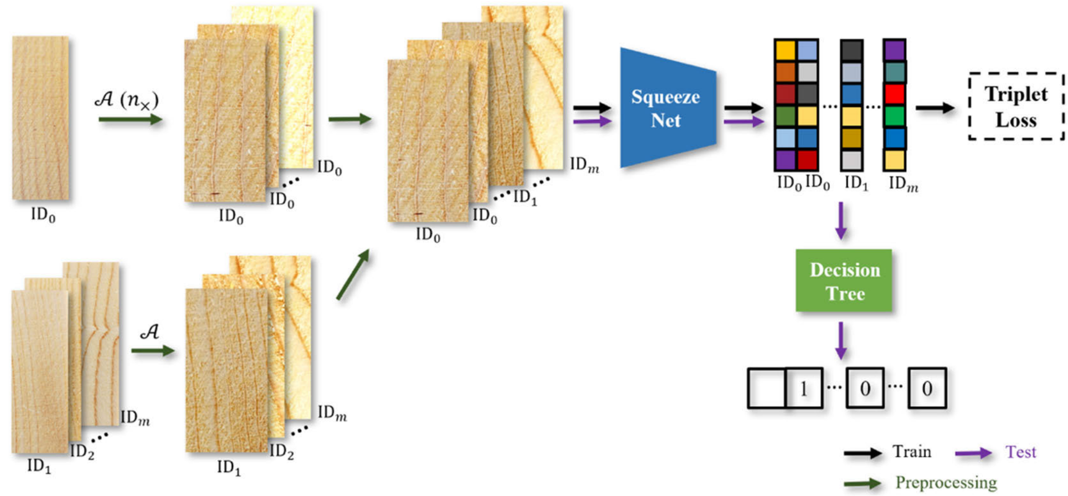

FIGURE 4. A schematic diagram illustrating the constructing process of a deep Squeeze-Net models for wood recognition. Here A stands for data augmentation, ID denotes identity. "1" is for "same" identity with the first sample (ID0), "0" is for "different" identity classification.

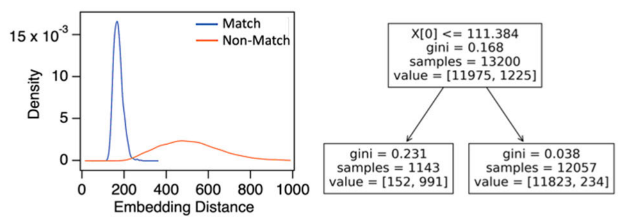

FIGURE 5. Left is the probability density of distance distribution from the trained model for same-identity and different-identity pairs in the training set. The curves show match rate and nonmatch rate for a given threshold α over the embedding distance distributions. Right is the decision tree visualization: The value 111.384 is the threshold value we obtained. This value was used for the predictions in validation/test set.

FIGURE 6. Results of recognition on wood biometric images, including correctly recognized a), b), c) and misclassified wood images d), e). The higher label is "ground-truth → prediction". 1: same, 0: different. Dist: distance.

Match rate is the percentage of match pairs whose embedding distance are less than or equal to α, nonmatch rate is the percentage of nonmatch pairs whose embedding distance is less than α. The value of 111.384 is the threshold value we obtained. We use this value for the predictions in the validation or test set.

Four metrics are used as indicators to evaluate the performance of plant biometric recognition. The accuracy (ξ) is defined based on the percentage of correctly verified true positives (TP) and true negatives (TN) over the total verified samples, including false positives (FP) and false negatives (FN) as shown in Eq. 2, precision, recall, and F1 score can be calculated based on Eqs. 3, 4 and 5:

$$\xi = \frac{TP + TN}{TP + FP + FN + TN} \times 100\% \tag{2}$$

$$\text{Precision} = \frac{TP}{TP + FP} \times 100\% \tag{3}$$

$$\text{Recall} = \frac{TP}{TP + FN} \times 100\% \tag{4}$$

$$\text{F1score} = \frac{2 \times \text{Precision} \times \text{Recall}}{\text{Precision} + \text{Recall}} \times 100\% \tag{5}$$

where precision represents the positive predictive value, recall stands for the sensitivity of the system.

Figure 6 depicts the correctly recognized and misclassified wood samples whose accuracy is 96.06%. The higher label is "ground-truth → prediction". Figure 6 d) and e) are examples of the wrong classification, which indicates that the network is not able to 100% precisely predict the result. This results in incorrect identification of the wood key.

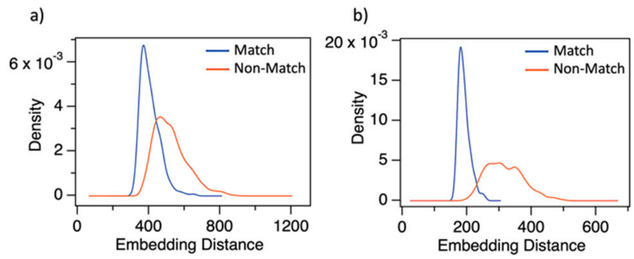

FIGURE 7. Results of recognition on leaf biometric images, including correctly recognized a), b), c) and misclassified d), e) leaf images. The higher label is "ground-truth → prediction". 1: same, 0: different. Dist: distance.

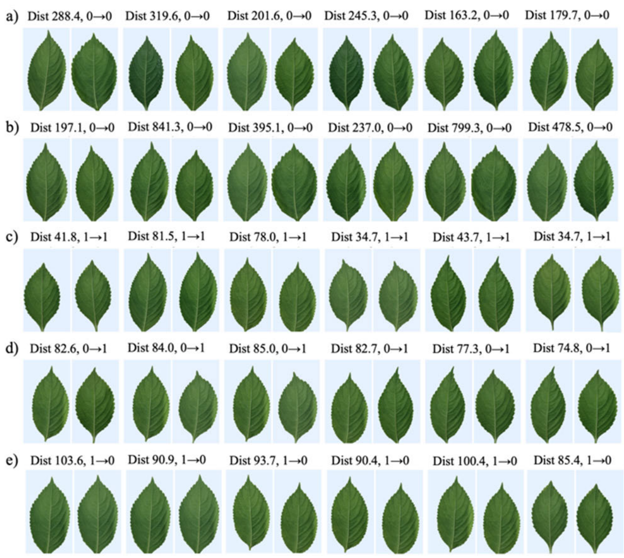

FIGURE 8. a) and d) are cosine distance distributions of different loss functions on CCLAS dataset. Genuine and imposter distributions are shown in blue and orange, respectively. The network on b) achives the best separation of the genuine/imposter score distributions. a) without the whole shape considered. b) with shape considered.

TABLE 1. Results of SCS biometric recognition.

	Accuracy	Precision	recall	F1 score
Wood Val - Less Data Augmentation	96.75%	57.71%	73.00%	64.46%
Wood Test - Less Data Augmentation	96.48%	55.37%	67.00%	60.63%
Wood Val - More Data Augmentation	96.69%	55.56%	90.00%	68.70%
Wood Test - More Data Augmentation	96.63%	55.08%	89.50%	68.19%
Wood Val - Large α	97.56%	65.02%	85.50%	73.87%
Wood Test - Large α	96.06%	50.70%	91.00%	65.12%

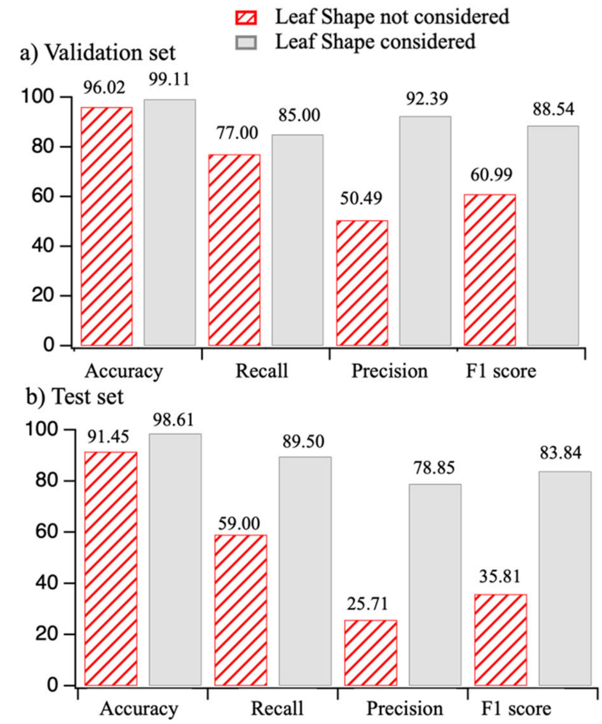

FIGURE 9. Comparison of leaf biometric recognition using CNN with validation set a), and test set b).

The sensitivity (recall) of the SCS dataset can be ameliorated from 67.00% to 89.50% for the test set simply by applying more data augmentation, while simultaneously F1 score is improved from 60.63% to 68.19% (Table 1). However, there is no obvious difference between the four metrics with or without using a large margin.

Figure 7 shows some examples of correctly and falsely recognized leaf images, including the true negative and true positive samples in a), b), and c). The matching is performed by establishing feature correspondences based on their deep embeddings.

Figure 8 depicts the genuine or imposter cosine distance distributions on the CCLAS validation and test sets. Kernel Density Estimation (KDE) is applied to measure the probability density of cosine distances. From figure 8 a), we can see a large overlap between the genuine and imposter distribution curves. This implies that some features of different leaf keys are incredibly close, leading to a low positive predictive value (precision). A clear separation can be observed between the two curves in Figure 8 b), this is consistent with the good performance evaluated by metrics.

To increase the reliability of the leaf biometric system, the performance of the leaf biometric network is studied with and without considering the leaf shape parameter. We found that after considering the whole leaf shape, the network has outperformed the previous one by an improvement of 7.1% in accuracy, 50.0% in F1 score, 30.5% in precision, and 53.1% in recall. This works both in the validation set and the test set. The system was designed such that it was able to achieve three main things; recognize with 99.11% accuracy and an f1 score of 88.54%, recognize and identify its type with 98.61% accuracy and an f1 score of 89.50%. The graph shown in Figure 9 illustrates the results in further detail.

Table 2 demonstrates that our system has achieved an accuracy value that surpasses the majority of previously reported systems in terms of accuracy. Notably, numerous studies focusing on wood or leaf recognition have reported systems

TABLE 2. Comparison of the results obtained from our system (in bold) with those reported in state-of-the-art publications.

Object	Method	Accuracy	Reference
Wood (Pine)	Artificial Neural Network	81.2 %	[53]
Wood (Pine)	Sum of Squared Differences + Speeded-Up Robust Features	90 %	[54]
Wood (Salix)	Support Vector Machine	95.2 %	[55]
Wood	Extreme Learning Machine	93.07%	[56]
Wood	CNN	93.4 %	[57]
Wood	CNN	80.3 %	[58]
Wood	CNN	94.9 %	[29]
Wood	Artificial Neural Networks	94 %	[59]
Wood (Spruce)	**CNN**	**96.06 %**	**Our work**
Leaf	Integral Contour Angles	98.4 %	[60]
Leaf	Shape Based Image Retrieval	90 %	[61]
Leaf	Curvilinear Shape Descriptor	72.22 %	[62]
Leaf	Scale Invariant Feature Transform	87.5 %	[42]
Leaf (Rice)	CNN	97 %	[30]
Leaf (Betel)	CNN	96.02 %	[63]
Leaf	CNN	95 %	[64]
Leaf (Maize)	CNN	96.5 %	[65]
Leaf (Richweed)	**CNN**	**98.61 %**	**Our work**

consistent with the good performance evaluated by metrics.

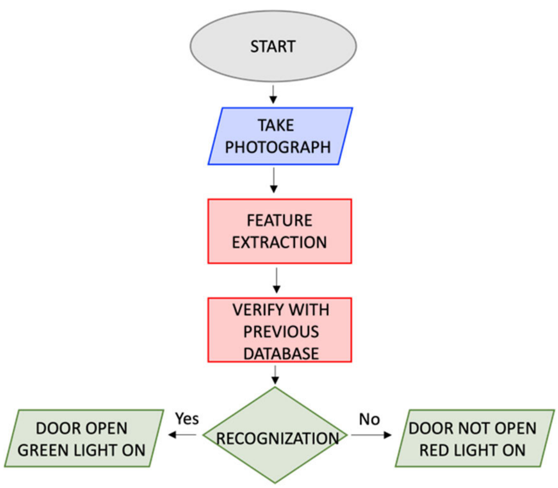

FIGURE 10. Diagram for the whole application setup.

for species recognition or classification. In such cases, the variations between different species are considerably larger than the differences within the same species. Our accuracy values (96.06% for wood and 98.61% for leaf) are based on discerning differences within the same species, including instances where the samples were taken from the same trunk with a vertical distance of just 5 cm, as explained in Part III. A.

V. APPLICATION AND DISCUSSION

Figure 10 and 11 illustrates a proof-of-concept application that involves a camera system, a Python CNN system, and a Python lock. The camera captures images, specifically of wood, and extracts the encodings of the wood biometric feature. These encodings are then compared to those stored in the database for verification. If the encoding matches ($\alpha \leq 111.384$), the green light turns on, indicating that the door is opened. Conversely, if the wood feature is unknown ($\alpha > 111.384$), the red light turns on, indicating that the door remains closed.

The verification process is documented, and the corresponding distance value is displayed on the CNN network. Figure 11b shows a screenshot of the output. In the first section, 10 wood blocks are designed as "false keys" that do not match, while one wood block is defined as the "correct key" that matches the stored encodings. By using the "correct key," the green light is automatically turned on, indicating a successful door opening. However, if any of the 10 "wrong keys" are used, the red light is illuminated.

In the second section, the system verifies the repositioning of the "correct key" and the upside-down placement of the "wrong keys." This further demonstrates the reliability of the system in correctly identifying the wood feature and distinguishing between the correct and incorrect keys.

While using wood or leaf biometrics for authentication in a lock system may offer certain advantages such as natural and renewable features, it also presents several challenges and disadvantages that need to be carefully considered before implementation. Firstly, Wood and leaves can be affected by environmental conditions such as humidity, temperature, and natural decay. These factors can alter the biometric characteristics of the material, potentially leading to false readings or inconsistencies in authentication. Secondly, Wood and leaves can deteriorate over time, especially when exposed to outdoor or harsh conditions. This can lead to changes in their biometric characteristics, affecting the accuracy of authentication.

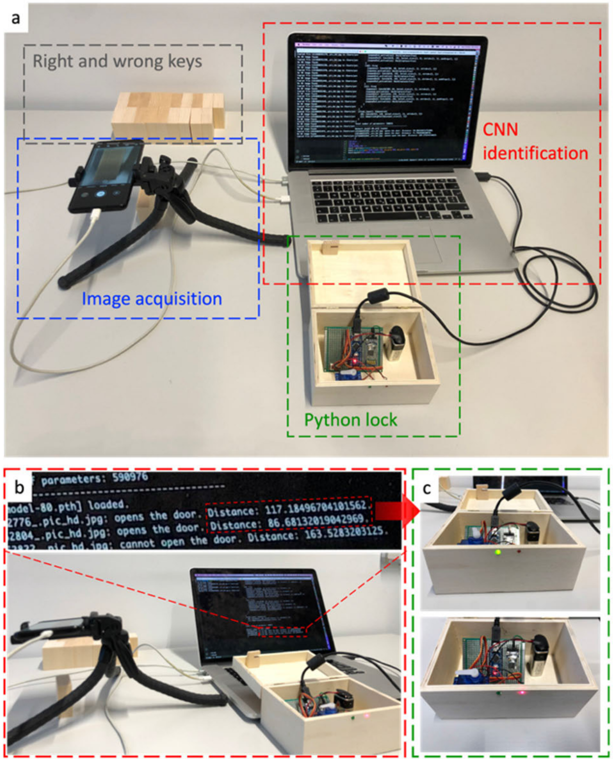

FIGURE 11. Examplenary application setup of wood biometric authentication system. a) Overview of the four composites: keys, image aquasition, CNN indentification implemented in Python, a lock controlled by Python. b) a switch order sent from Python depended on distance value. c) Green light represents for "open the door", red light means "not open the door."

Additionally, wear and tear can occur with repeated use, potentially rendering the biometric data less reliable or ineffective. Therefore, a proper encapsulation process is necessary for successfully commercialization in real-world applications commercialization in real application scenario.

VI. CONCLUSION

Considering the increasing fraudulent use and other legal issues of applications related to human biometric authentication, there exists a need for employing an alternative system to protect human biometric information. In this paper, we implemented a deep learning technique, CNN, for the recognition and identification of wood and leaf biometric patterns. The proposed system was trained and tested using the datasets, and the experimental results deduced indicate the feasibility and effectiveness of using plant-based biometric patterns in conjunction with CNN in a authentication system. In a nutshell, both wood and leaf biometric recognition systems result in accuracy values above 96% in the validation set and the test set. The application further demonstrates its high reliability and practicability in real-world scenarios.

ACKNOWLEDGMENT

(Wenqing Yan and Jingwei Tang contributed equally to this work.)

REFERENCES

[1] S. Vhaduri, S. V. Dibbo, and W. Cheung, "HIAuth: A hierarchical implicit authentication system for IoT wearables using multiple biometrics," *IEEE Access*, vol. 9, pp. 116395–116406, 2021, doi: 10.1109/ACCESS.2021.3105481.

[2] M. L. Ali, K. Thakur, C. C. Tappert, and M. Qiu, "Keystroke biometric user verification using hidden Markov model," in *Proc. IEEE 3rd Int. Conf. Cyber Secur. Cloud Comput. (CSCloud), 2nd IEEE Int. Conf. Scalable Smart Cloud (IEEE SSC)*, Beijing, China, Jun. 2016, pp. 204–209, doi: 10.1109/CSCloud.2016.23.

[3] G. S. Eskander, R. Sabourin, and E. Granger, "A bio-cryptographic system based on offline signature images," *Inf. Sci.*, vol. 259, pp. 170–191, Feb. 2014, doi: 10.1016/j.ins.2013.09.004.

[4] A. Kholmatov and B. Yanikoglu, "Biometric cryptosystem using online signatures," in *21st Int. Symp. Comput. Inf. Sci. (ISCIS)*, in Lecture Notes in Computer Science, vol. 4263, İstanbul, Turkey, Nov. 2006, p. 981.

[5] J. Baidya, T. Saha, R. Moyashir, and R. Palit, "Design and implementation of a fingerprint based lock system for shared access," in *Proc. IEEE 7th Annu. Comput. Commun. Workshop Conf. (CCWC)*, Las Vegas, NV, USA, Jan. 2017, pp. 1–6.

[6] I. F. Ismail, M. Fawzi, W. A. W. Jamaludin, R. H. Madon, A. F. Abdullah, and M. A. Abdullah, "Development of a lock biometric authentication system for a battery powered locking device," *Int. J. Integr. Eng.*, vol. 13, no. 2, pp. 16–23, 2021.

[7] M. Szczepanik, I. J. Jozwiak, T. Jamka, and K. Stasinski, "Security lock system for mobile devices based on fingerprint recognition algorithm," in *Proc. 36th Int. Conf. Inf. Syst. Archit. Technol. (ISAT)*, in Advances in Intelligent Systems and Computing, vol. 431, Karpacz, Poland, Sep. 2015, pp. 25–35, doi: 10.1007/978-3-319-28564-1_3.

[8] M. Doi, Q. Chen, K. Sato, and K. Chihara, "Lock-control system using face identification," in *Audio- and Video-based Biometric Person Authentication* (Lecture Notes in Computer Science), vol. 1206, J. Bigun, G. Chollet, and G. Borgefors, Eds. Berlin, Germany: Springer-Verlag, 1997, pp. 361–368.

[9] T. Ko, "Iris recognition for biometric identification," in *Proc. 9th World Multi-Conf. Syst., Cybern. Inform.*, Orlando, FL, USA, Jul. 2005, pp. 263–268.

[10] P. P. Polash and M. M. Monwar, "Human iris recognition for biometric identification," in *Proc. 10th Int. Conf. Comput. Inf. Technol.* Dhanmondi, Bangladesh: United International University, Dec. 2007, p. 44.

[11] O. Seyeddain, H. Kraker, A. Redlberger, A. K. Dexl, G. Grabner, and M. Emesz, "Reliability of automatic biometric iris recognition after phacoemulsification or drug-induced pupil dilation," *Eur. J. Ophthalmol.*, vol. 24, no. 1, pp. 58–62, Jan. 2014, doi: 10.5301/ejo.5000343.

[12] A. Alruwaili and S. Hendaoui, "Improved multi-layer authentication scheme by merging one-time password with voice biometric factor," *Int. J. Comput. Sci. Netw. Secur.*, vol. 21, no. 9, pp. 346–353, Sep. 2021, doi: 10.22937/ijcsns.2021.21.9.45.

[13] M. Ghalandari, I. Mahariq, F. Ghadak, O. Accouche, and F. Jarad, "Dynamic audio-visual biometric fusion for person recognition," *Comput., Mater. Continua*, vol. 71, no. 1, pp. 1283–1311, 2022, doi: 10.32604/cmc.2022.021608.

[14] R. A. Rashid, N. H. Mahalin, M. A. Sarijari, and A. A. A. Aziz, "Security system using biometric technology: Design and implementation of voice recognition system (VRS)," in *Proc. Int. Conf. Comput. Commun. Eng.*, Kuala Lumpur, Malaysia, May 2008, pp. 898–902, doi: 10.1109/iccce.2008.4580735.

[15] Experian. (2021). *2021 Global Identity and Fraud Report*. [Online]. Available: https://www.experian.de/content/dam/noindex/emea/germany/Experian-Global-Identity-Fraud-Report-2021.pdf

[16] M. Smith and S. Miller, "The ethical application of biometric facial recognition technology," *AI Soc.*, vol. 37, no. 1, pp. 167–175, Mar. 2022, doi: 10.1007/s00146-021-01199-9.

[17] F. M. Z. Heravi, E. Farazdaghi, R. Fournier, and A. Nait-Ali, "Impact of aging on three-dimensional facial verification," *Electronics*, vol. 8, no. 10, Oct. 2019, Art. no. 1170, doi: 10.3390/electronics8101170.

[18] S.-W. Hwang and J. Sugiyama, "Computer vision-based wood identification and its expansion and contribution potentials in wood science: A review," *Plant Methods*, vol. 17, no. 1, Apr. 2021, Art. no. 47, doi: 10.1186/s13007-021-00746-1.

[19] S. Sachar and A. Kumar, "Survey of feature extraction and classification techniques to identify plant through leaves," *Expert Syst. Appl.*, vol. 167, Apr. 2021, Art. no. 114181, doi: 10.1016/j.eswa.2020.114181.

[20] G. Koch, I. Heinz, and H. G. Richter, "Demonstration of the database macroHOLZdata computer-aided identification and description of trade timbers," in *Proc. 8th Hardwood Conf. New Aspects Hardwood Utilization, From Sci. Technol.*, Sopron, Hungary, Oct. 2018, pp. 72–73.
[21] J. Y. Tou, Y. H. Tay, and P. Y. Lau, "Rotational invariant wood species recognition through wood species verification," in *Proc. 1st Asian Conf. Intell. Inf. Database Syst.*, Dong Hoi, Vietnam, Apr. 2009, pp. 115–120, doi: 10.1109/aciids.2009.10.
[22] A. R. de Geus, S. F. D. Silva, A. B. Gontijo, F. O. Silva, M. A. Batista, and J. R. Souza, "An analysis of timber sections and deep learning for wood species classification," *Multimedia Tools Appl.*, vol. 79, nos. 45–46, pp. 34513–34529, Dec. 2020, doi: 10.1007/s11042-020-09212-x.
[23] H.-J. Wang, H.-N. Qi, and X.-F. Wang, "A new Gabor based approach for wood recognition," *Neurocomputing*, vol. 116, pp. 192–200, Sep. 2013, doi: 10.1016/j.neucom.2012.02.045.
[24] S. Mouine, I. Yahiaoui, and A. Verroust-Blondet, "Combining leaf salient points and leaf contour descriptions for plant species recognition," in *Proc. 10th Int. Conf. Image Anal. Recognit. (ICIAR)*, in Lecture Notes in Computer Science, vol. 7950, Povoa de Varzim, Portugal, Jun. 2013, pp. 205–214.
[25] R. Schraml, J. Charwat-Pessler, and A. Uhl, "Temporal and longitudinal variances in wood log cross-section image analysis," in *Proc. IEEE Int. Conf. Image Process. (ICIP)*, Paris, France, Oct. 2014, pp. 5706–5710.
[26] R. Schraml, J. Charwat-Pessler, A. Petutschnigg, and A. Uhl, "Towards the applicability of biometric wood log traceability using digital log end images," *Comput. Electron. Agricult.*, vol. 119, pp. 112–122, Nov. 2015, doi: 10.1016/j.compag.2015.10.003.
[27] G. Wimmer, R. Schraml, H. Hofbauer, A. Petutschnigg, and A. Uhl, "Two-stage CNN-based wood log recognition," in *Proc. 21st Int. Conf. Comput. Sci. Appl. (ICCSA)*, in Lecture Notes in Computer Science, vol. 12955, Cagliari, Italy, Sep. 2021, pp. 115–125, doi: 10.1007/978-3-030-87007-2_9.
[28] X. YongHua and W. Jin-Cong, "Study on the identification of the wood surface defects based on texture features," *Optik*, vol. 126, no. 19, pp. 2231–2235, Oct. 2015, doi: 10.1016/j.ijleo.2015.05.101.
[29] J. Huang, X. Lu, L. Chen, H. Sun, S. Wang, and G. Fang, "Accurate identification of pine wood nematode disease with a deep convolution neural network," *Remote Sens.*, vol. 14, no. 4, Feb. 2022, Art. no. 913, doi: 10.3390/rs14040913.
[30] S. M. M. Hossain, M. M. M. Tanjil, M. A. B. Ali, M. Z. Islam, M. S. Islam, S. Mobassirin, I. H. Sarker, and S. M. R. Islam, "Rice leaf diseases recognition using convolutional neural networks," in *Proc. 16th Int. Conf. Adv. Data Mining Appl. (ADMA)*, in Lecture Notes in Artificial Intelligence, vol. 12447, Foshan, China, Nov. 2020, pp. 299–314, doi: 10.1007/978-3-030-65390-3_23.
[31] S. Zhang, W. Huang, and C. Zhang, "Three-channel convolutional neural networks for vegetable leaf disease recognition," *Cogn. Syst. Res.*, vol. 53, pp. 31–41, Jan. 2019, doi: 10.1016/j.cogsys.2018.04.006.
[32] M. Verheyen, W. Beckers, E. Claesen, G. Moonen, and E. Demeester, "Vision-based sorting of medium density fibreboard and grade a wood waste," in *Proc. IEEE 21st Int. Conf. Emerg. Technol. Factory Autom. (ETFA)*. Berlin, Germany: OWL Univ. of Applied Sciences and Arts, Sep. 2016, pp. 1–6.
[33] K. Kobayashi, M. Akada, T. Torigoe, S. Imazu, and J. Sugiyama, "Automated recognition of wood used in traditional Japanese sculptures by texture analysis of their low-resolution computed tomography data," *J. Wood Sci.*, vol. 61, no. 6, pp. 630–640, Dec. 2015, doi: 10.1007/s10086-015-1507-6.
[34] B. G. de Andrade, V. M. Basso, and J. V. de Figueiredo Latorraca, "Machine vision for field-level wood identification," *IAWA J.*, vol. 41, no. 4, pp. 681–698, Jun. 2020, doi: 10.1163/22941932-bja10001.
[35] R. Yusof, M. Khalid, and A. S. M. Khairuddin, "Application of kernel-genetic algorithm as nonlinear feature selection in tropical wood species recognition system," *Comput. Electron. Agricult.*, vol. 93, pp. 68–77, Apr. 2013, doi: 10.1016/j.compag.2013.01.007.
[36] P. M. Devi and M. Sornam, "Classification of ancient handwritten Tamil characters on palm leaf inscription using modified adaptive backpropagation neural network with GLCM features," *ACM Trans. Asian Low-Resour. Lang. Inf. Process.*, vol. 19, no. 6, pp. 1–24, Nov. 2020, doi: 10.1145/3406209.
[37] M. Nasirzadeh, A. A. Khazael, and M. B. Khalid, "Woods recognition system based on local binary pattern," in *Proc. 2nd Int. Conf. Comput. Intell., Commun. Syst. Netw.*, Liverpool, U.K., Jul. 2010, pp. 308–313, doi: 10.1109/CICSyN.2010.27.
[38] J. Martins, L. S. Oliveira, S. Nisgoski, and R. Sabourin, "A database for automatic classification of forest species," *Mach. Vis. Appl.*, vol. 24, no. 3, pp. 567–578, Apr. 2013, doi: 10.1007/s00138-012-0417-5.
[39] Z. Lv and Z. Zhang, "Research on plant leaf recognition method based on multi-feature fusion in different partition blocks," *Digit. Signal Process.*, vol. 134, Apr. 2023, Art. no. 103907, doi: 10.1016/j.dsp.2023.103907.
[40] K. Kobayashi, T. Kegasa, S.-W. Hwang, and J. Sugiyama, "Anatomical features of *Fagaceae* wood statistically extracted by computer vision approaches: Some relationships with evolution," *PLoS ONE*, vol. 14, no. 8, Aug. 2019, Art. no. e0220762, doi: 10.1371/journal.pone.0220762.
[41] P. Barmpoutis, K. Dimitropoulos, I. Barboutis, N. Grammalidis, and P. Lefakis, "Wood species recognition through multidimensional texture analysis," *Comput. Electron. Agricult.*, vol. 144, pp. 241–248, Jan. 2018, doi: 10.1016/j.compag.2017.12.011.
[42] S. Lavania and P. S. Matey, "Leaf recognition using contour based edge detection and SIFT algorithm," in *Proc. IEEE Int. Conf. Comput. Intell. Comput. Res.* Coimbatore, India: Park College of Engineering and Technology, Dec. 2014, pp. 275–278.
[43] S.-W. Hwang, K. Kobayashi, and J. Sugiyama, "Detection and visualization of encoded local features as anatomical predictors in cross-sectional images of *Lauraceae*," *J. Wood Sci.*, vol. 66, no. 1, Mar. 2020, Art. no. 16, doi: 10.1186/s10086-020-01864-5.
[44] M. F. Kazerouni, J. Schlemper, and K. D. Kuhnert, "Automatic plant recognition system for challenging natural plant species," in *Proc. 25th Int. Conf. Central Eur. Comput. Graph., Vis. Comput. Vis. (WSCG)*, in Computer Science Research Notes, vol. 2702, Pilsen, Czech Republic, May/Jun. 2017, pp. 81–90.
[45] Y. Yang, X. Zhou, Y. Liu, Z. Hu, and F. Ding, "Wood defect detection based on depth extreme learning machine," *Appl. Sci.*, vol. 10, no. 21, p. 7488, Oct. 2020, doi: 10.3390/app10217488.
[46] Z. Zhao, X. Yang, Z. Ge, H. Guo, and Y. Zhou, "Wood microscopic image identification method based on convolution neural network," *BioResources*, vol. 16, no. 3, pp. 4986–4999, May 2021, doi: 10.15376/biores.16.3.4986-4999.
[47] R. L. Jyothi and M. A. Rahiman, "A multilevel CNN architecture for character recognition from palm leaf images," in *Proc. 3rd Int. Conf. Intell. Comput. Commun. (ICICC)*, in Advances in Intelligent Systems and Computing, vol. 1034. Bengaluru, India: Dayananda Sagar Univ., 2020, pp. 185–193, doi: 10.1007/978-981-15-1084-7_19.
[48] A. Krizhevsky, I. Sutskever, and G. E. Hinton, "ImageNet classification with deep convolutional neural networks," *Commun. ACM*, vol. 60, no. 6, pp. 84–90, May 2017, doi: 10.1145/3065386.
[49] K. Simonyan and A. Zisserman, "Very deep convolutional networks for large-scale image recognition," 2014, *arXiv:1409.1556*.
[50] B. Li, W. Wei, A. Ferreira, and S. Tan, "ReST-Net: Diverse activation modules and parallel subnets-based CNN for spatial image steganalysis," *IEEE Signal Process. Lett.*, vol. 25, no. 5, pp. 650–654, May 2018.
[51] F. N. Iandola, S. Han, M. W. Moskewicz, K. Ashraf, W. J. Dally, and K. Keutzer, "SqueezeNet: AlexNet-level accuracy with 50× fewer parameters and <0.5 MB model size," 2016, *arXiv:1602.07360*.
[52] K. Q. Weinberger and L. K. Saul, "Distance metric learning for large margin nearest neighbor classification," *J. Mach. Learn. Res.*, vol. 10, pp. 207–244, Jun. 2009.
[53] L. G. Esteban, P. de Palacios, M. Conde, F. G. Fernández, A. García-Iruela, and M. González-Alonso, "Application of artificial neural networks as a predictive method to differentiate the wood of *Pinus sylvestris* L. and *Pinus nigra* Arn subsp. *salzmannii* (Dunal) Franco," *Wood Sci. Technol.*, vol. 51, no. 5, pp. 1249–1258, Sep. 2017, doi: 10.1007/s00226-017-0932-7.
[54] T. Pahlberg, O. Hagman, and M. Thurley, "Recognition of boards using wood fingerprints based on a fusion of feature detection methods," *Comput. Electron. Agricult.*, vol. 111, pp. 164–173, Feb. 2015, doi: 10.1016/j.compag.2014.12.014.
[55] K. Turhan and B. Serdar, "Support vector machines in wood identification: The case of three Salix species from Turkey," *Turkish J. Agricult. Forestry*, pp. 249–256, Jan. 2013, doi: 10.3906/tar-1205-47.
[56] P. Huang, F. Zhao, Z. Zhu, Y. Zhang, X. Li, and Z. Wu, "Application of variant transfer learning in wood recognition," *BioResources*, vol. 16, no. 2, pp. 2557–2569, Feb. 2021, doi: 10.15376/biores.16.2.2557-2569.
[57] P. P. Htun, M. Boschetti, A. Buriro, R. Confalonieri, B. Sun, A. N. Htwe, and T. Tillo, "A lightweight approach for wood hyperspectral images classification," in *Proc. IEEE Int. Conf. Multimedia Expo Workshops (ICMEW)*, Jul. 2021, pp. 1–4, doi: 10.1109/ICMEW53276.2021.9455943.

[58] G. Figueroa-Mata, E. Mata-Montero, J. C. Valverde-Otárola, D. Arias-Aguilar, and N. Zamora-Villalobos, ''Using deep learning to identify Costa Rican native tree species from wood cut images,'' *Frontiers Plant Sci.*, vol. 13, Apr. 2022, Art. no. 789227, doi: 10.3389/fpls.2022.789227.

[59] G. de Souza Vieira, M. M. D. Ponte, V. P. Moutinho, R. Jardim-Gonçalves, C. P. Lima, and M. de Albuquerque Vinagre, ''Identification of wood from the Amazon by characteristics of Haralick and neural network: Image segmentation and polishing of the surface,'' *iForest, Biogeosci. Forestry*, vol. 15, no. 4, pp. 234–239, Aug. 2022, doi: 10.3832/ifor3906-015.

[60] F. Ni and B. Wang, ''Integral contour angle: An invariant shape descriptor for classification and retrieval of leaf images,'' in *Proc. 25th IEEE Int. Conf. Image Process. (ICIP)*, Athens, Greece, Oct. 2018, pp. 1223–1227.

[61] C. Caballero and M. C. Adranda, ''Plant species identification using leaf image retrieval,'' in *Proc. ACM Int. Conf. Image Video Retr. (CIVR)*, 2010, pp. 327–334.

[62] Y. Herdiyeni, D. I. Lubis, and S. Douady, ''Leaf shape identification of medicinal leaves using curvilinear shape descriptor,'' in *Proc. 7th Int. Conf. Soft Comput. Pattern Recognit. (SoCPaR)*. Fukuoka, Japan: Kyushu Univ., Nov. 2015, pp. 218–223.

[63] R. H. Hridoy, T. Habib, I. Jabiullah, R. Rahman, and F. Ahmed, ''Early recognition of betel leaf disease using deep learning with depth-wise separable convolutions,'' in *Proc. IEEE Region 10 Symp. (TENSYMP)*. Jeju, South Korea: Good Technologies for Creating Future, Aug. 2021, pp. 1–7, doi: 10.1109/TENSYMP52854.2021.9551009.

[64] T. K. N. Thanh, Q. B. Truong, Q. D. Truong, and H. H. Xuan, ''Depth learning with convolutional neural network for leaves classifier based on shape of leaf vein,'' in *Proc. 10th Asian Conf. Intell. Inf. Database Syst. (ACIIDS)*, in Lecture Notes in Artificial Intelligence, vol. 10751, Dong Hoi, Vietnam, Mar. 2018, pp. 565–575, doi: 10.1007/978-3-319-75417-8_53.

[65] K. Sentamilselvan, M. H. Rithanya, T. V. Dharshini, S. Kumar, and R. Aarthi, ''Maize leaf disease detection using convolutional neural network,'' in *Proc. 3rd Doctoral Symp. Comput. Intell. (DoSCI)*, in Lecture Notes in Networks and Systems, vol. 479. Lucknow, India: Institution of Engineering and Technology, Mar. 2022, 2023, pp. 247–260, doi: 10.1007/978-981-19-3148-2_21.

WENQING YAN (Member, IEEE) received the B.S. degree in materials science and chemistry from Northwest University, Xi'an, China, in 2013, the M.S. degree in polymer science from the University of Freiburg, Freiburg, Germany, in 2017, and the Ph.D. degree in materials science from ETH Zürich, Zürich, Switzerland, in 2020. She is currently a Senior Researcher with the Department of Civil, Environmental and Geomatic Engineering, ETH Zürich. Her research interests include polymerization mechanisms, advanced image processing and analysis, as well as digital image correlation and tracking.

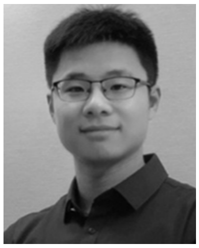

JINGWEI TANG received the B.S. degree in physics from Nanjing University, Nanjing, China, in 2016, and the M.S. degree in computational science and engineering and the Ph.D. degree in computer science from ETH Zürich, Zürich, Switzerland, in 2018 and 2022, respectively. Since 2022, he has been an Associate Research Scientist with DisneyResearch|Studios, Zürich. His research interests include physics-based simulations for computer graphics, machine learning, and deep learning techniques, with a focus on artistic simulation controls. He was a recipient of the Günther Enderle Best Paper Award from Eurographics 2021.

SANDRO STUCKI received the B.S. degree in food technology from the Zurich University of Applied Sciences (ZHAW), in 2014, and the M.S. degree in food science from the Swiss Federal Institute of Technology (ETH Zürich), Switzerland, in 2017. He is currently pursuing the Ph.D. degree with the Wood Material Science Group, ETH Zürich, and the Cellulose and Wood Materials Group, Swiss Federal Laboratories for Materials Science and Technology (Empa), Switzerland, under the supervision of Prof. Dr. Ingo Burgert. In 2018, he was a Research Assistant with the Soft Materials Laboratory, ETH Zürich. His research interests include novel glueing techniques and wood-based composites, with a focus on characterizing and improving the moisture stability of bonded wood joints.